Taylor & Francis
Taylor & Francis Group

Automatika

Journal for Control, Measurement, Electronics, Computing and Communications

ISSN: (Print) (Online) Journal homepage: www.tandfonline.com/journals/taut20

Probe card-Type multizone electrostatic chuck inspection system

Yoon Sung Koo, Jae Hwan Kim, Chan Su Han & Sang Jeen Hong

To cite this article: Yoon Sung Koo, Jae Hwan Kim, Chan Su Han & Sang Jeen Hong (2023) Probe card-Type multizone electrostatic chuck inspection system, Automatika, 64:2, 389-398, DOI: 10.1080/00051144.2023.2169157

To link to this article: https://doi.org/10.1080/00051144.2023.2169157

Published online: 23 Jan 2023.

AUTOMATIKA
2023, VOL. 64, NO. 2, 389–398
https://doi.org/10.1080/00051144.2023.2169157

REGULAR PAPER

OPEN ACCESS Check for updates

Probe card-Type multizone electrostatic chuck inspection system

Yoon Sung Koo, Jae Hwan Kim, Chan Su Han and Sang Jeen Hong

Department of Electronics Engineering, Myongji University, Yongin, Republic of Korea

ABSTRACT

Electrostatic chucks (ESCs) are major components of the equipment used to improve the production yield of wafers and temperature uniformity across wafer surfaces by controlling the wafer temperature precisely. However, ESCs are directly exposed to harsh environments, such as plasma, chemical gases, and high temperature fluctuations. Therefore, ESCs may malfunction if used for a certain period. Therefore, repair and performance verification of failed ESCs are required. In this study, we developed a multizone probe card system suitable for electrical testing of the heating electrodes embedded in ESC control modules to correlate the failure mode factors of ESCs. This system has the advantages of examining the resistance of the internal heating electrode of a 144-zone ESC in a short time and detecting an abnormality in this component based on the measured data. The heating electrode resistance measurement error rate of the developed system was 1%, and the maintenance time was reduced by approximately 66% compared with that of existing ESC maintenance methods.

ARTICLE HISTORY
Received 27 October 2021
Accepted 12 January 2023

KEYWORDS
Electrostatic chuck; probe card; heating electrode; resistance; testing

Introduction

Owing to the miniaturization and complex integration of semiconductor manufacturing processes, traditional planar-type device technology following Moore's law suffers from problems, such as short-channel effect and gate oxide control. Hence, three-dimensional (3D) structured devices have been developed. However, the overall process time is continuously increasing, and new technologies, such as high-aspect ratio etching, and high-level process control are required [1, 2]. Particularly, the temperature uniformity of a wafer surface affects the etch rate. Therefore, the temperature distribution must be the same at all positions on a wafer to obtain uniform process results [3, 4]. However, the process chamber has structural limitations, and the temperature distribution from the centre to the edge of a wafer is non-uniform. Therefore, an electrostatic chuck (ESC) is employed to achieve uniform temperature distribution over an entire wafer.

ESC significantly affects the surface temperature of a wafer inside the plasma process chamber. To increase the temperature uniformity of a wafer, ESC heating electrode should be changed from single-zone to multizone [5]. With a single-zone heater, temperature control at the centre of a wafer is dominant; however, temperature control at the edges is difficult. To control the temperature distribution more precisely, multizone ESC with multiple zone heaters, such as two- and four-zone heaters, has been developed. In multizone ESC with multiple heaters, there is a heating circuit that controls the temperature by supplying power to the heating electrode in each heating zone [6]. As the heating area is increased, the temperature uniformity of a wafer is increased. Therefore, various multizone ESCs are continuously being developed to enhance the temperature uniformity of wafers [7, 8].

ESCs are exposed to harsh environments, such as temperature rising and falling conditions, high vacuum, and plasma, which can cause physical damage. Particularly, the interface of an ESC experiencing repeated high-temperature variations undergoes exfoliation or cracking owing to the difference in the thermal expansion coefficients of the upper ceramic plate and heating electrode [9, 10]. Repeated temperature fluctuation affects the metal resistance component of the heating electrode. This lowers the temperature control function of the ESC, thereby reducing the temperature uniformity of a wafer. An ESC has individual heating areas of different sizes and a variable-length heating electrode, as shown in Figure 1. Therefore, the resistance component of the heating electrode varies in different locations. To repair an ESC whose temperature control function has degraded, the resistance of the heating electrode should be measured and evaluated [11]. During the measurement process, an operator manually measures the resistance of the heating electrode using a multimeter. As the number of heating zones increases, the time required to measure the resistance also increases. Moreover, a measurement error can result in incorrect diagnosis. Therefore, a system that can measure temperature promptly and accurately is required. In this study, we propose a probe card-type

CONTACT Sang Jeen Hong samhong@mju.ac.kr Department of Electronics Engineering, Myongji University, Yongin 17058, Republic of Korea

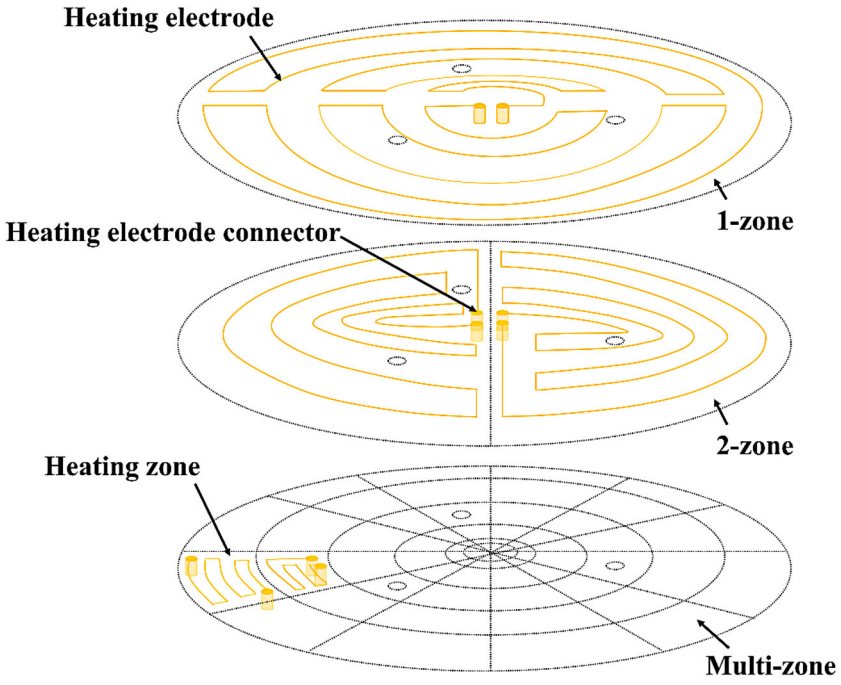

Figure 1. Drawing of ESC heating zones and heating electrodes.

inspection system suitable for functional testing of ESCs to reduce maintenance procedures. Increasing the heating zones of ESCs makes functional testing difficult during traditional maintenance. The proposed system has the advantages of inspecting the heating electrode resistance component of a multizone ESC faster than that required in traditional maintenance and determining whether the heating electrode is abnormal based on the acquired data. In the Measurement System Design section, we summarize the literature on the methods used for measuring heating electrode resistance in a multizone ESC and present the measurement methods, algorithms, and circuit designs used in this study. In the Experimental Apparatus section, we provide the experimental procedure for measuring the resistance of the heating electrode inside an ESC. The Results and Discussion section discusses the performance of the probe card system (PCS) according to the measured data. Finally, the Conclusion section presents the conclusion of this study.

Measurement system design

Generally, a probe card refers to a component used for equipment inspection that selects defective products by determining their electrical performance and identifying circuit failure by physically contacting the manufactured integrated circuit (IC) chip on a wafer. A probe card comprises of a thin wire probe attached to a specific standard circuit board. There are various types of probe cards, including horizontal, vertical, and micro electro-mechanical system [12, 13]. Multiple probe tips are required to inspect the manufactured chips on wafers. Different probe tips may be used depending on the test equipment. Digital control of multiple-channel multiplexers (MUXs) is required for efficient inspection [14]. The probe card developed in this study was designed on a printed circuit board (PCB) as it was confirmed to be suitable for measuring the resistance of ESC heating electrodes. Figure 2 shows a schematic of the probe card-type heating electrode resistance measurement system. The top-side ceramic

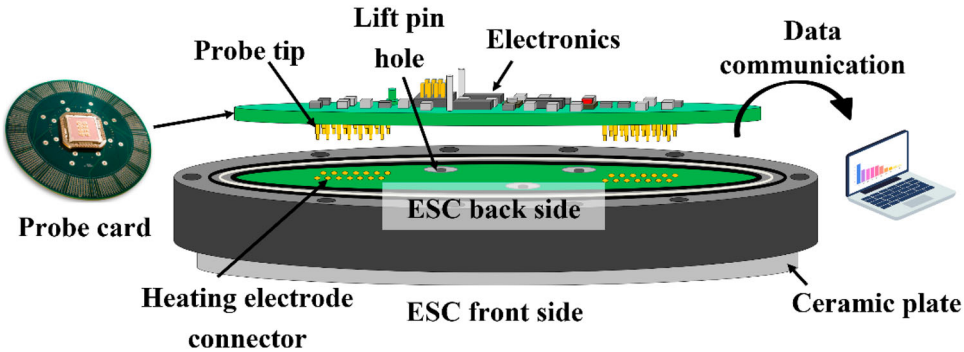

Figure 2. Schematic of ESC heating electrode resistance measurement system.

puck was debonded from the base metal plate of an ESC to be tested during the repair procedure to examine the heating electrode terminal on the backside [15]. Multiple probe tips were placed under the PCB based on the terminal position of the heating electrode. All probe tips were rounded to prevent damaging the heating electrode terminal, and all probe tips needed to be in contact with the terminal. A spring-type probe tip with a movement range of 1 mm was selected for all terminals to be in constant contact, and uniform contact with the heating electrode terminal was ensured. Each probe tip had a length of 6 mm and radius of 1.5 mm. To minimize physical scratches on the heating electrode connector of the test ESC, a round shape was selected for the contact area of the probe tip. The probe tip was finished with gold and nickel to allow electrical signals to pass through.

In the measurement system, a multiplexer, a microcontroller unit (MCU), MUXs, a regulator, a debugging port, and cables to receive the user input signals were set up on the top of the PCB. Several probe tips were located at the bottom of the PCB. Two probe tips measured the resistance of the heating electrode of the test ESC. The MCU controls the MUXs and selects the probe tip. The selected probe tips measure the resistance of the heating electrode using a digital multimeter (DMM) connected to the MUXs. The measured resistance is transmitted to a PC via a USB. The operation block diagram of the system is shown in Figure 3.

The heating mechanism of the heating electrode of an ESC follows Joule's law, which states that heat is generated when current is supplied to a metal body. Therefore, to heat a wafer, an electric current is supplied to the heating electrode in an ESC. However, when this current is delivered to the wafer, it can act as noise in the process plasma. Additionally, a high thermal conductivity material is required to uniformly heat the entire area of a wafer. Therefore, aluminum nitride and alumina were used as heating electrodes owing to their excellent electrical resistance and thermal conductivity

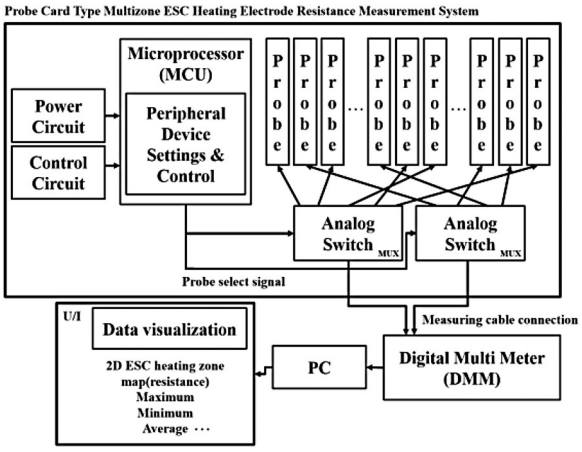

Figure 3. Block diagram of operation circuit.

Table 1. Classification of resistance.

Classification of resistance	Range	Measurement method
Low resistance	<1 Ω	Kelvin bridge and potentiometer method
Middle resistance	1 Ω–1 MΩ	Wheatstone bridge and voltage drop method
High resistance	>1 MΩ	Megger, intuitive method, and voltmeter method

[16]. The metal resistance of the heating electrode of an ESC follows the following relationship: $R = \rho L/A$, where ρ is the resistivity of the metal, L is the length of the metal line between two terminals, and A is the area. The resistance in the electric circuit prevents the flow of current and causes a voltage drop. The resistance between two points in the circuit can be expressed as a ratio of the voltage and current [17], and depending on its value, it is classified into low, medium, and high resistance. As summarized in Table 1, circuits can be measured precisely based on the resistance value. The resistance measurement range of an ESC heating electrode corresponds to the megaohm range, i.e. high resistance [18]. In this study, a DMM (*HIOKI's DT-4282*) with a built-in Megger circuit was used to accurately measure the resistance in megaohm using a 9.6 nA current source and internal reference resistance.

The ESC heating electrode resistance measurement system was designed using the layout tool of the EAGLE PCB design programme of Autodesk. First, a circuit was designed to measure the resistance of an ESC heating electrode using the EAGLE logic tool. Before creating the circuit diagram, components considering the actual environment and operating functions were selected. Two 16:1 MUXs (*ADG1606-Analog Device*) with a switching speed of 600 ns were used to rapidly control the multiple probe tips, and an MCU (*ADuCM362-3-Analog Device*) with an operating frequency of 16 MHz was selected to control the MUXs and process user signals. Designed for future use in actual equipment environments, the operating temperature of the electronic parts was ensured from −40 to 125 °C. The circuit diagram was designed by referring to the datasheet of the parts. Figure 4 shows the designed circuit diagram and PCB layout.

Experimental apparatus

An ESC comprises several complex layers, such as a ceramic plate on which a wafer is supported, an electrode that fixes the wafer with electrostatic force, and a heating electrode that raises the temperature. Additionally, it includes a He path that increases the heat transfer between the ESC and wafer and a cooling path that controls the temperature of the chuck. A cross-sectional view of the ESC structure is shown in Figure 5. The heating electrode of an ESC has a part that applies power to each zone, and the shape or position of the

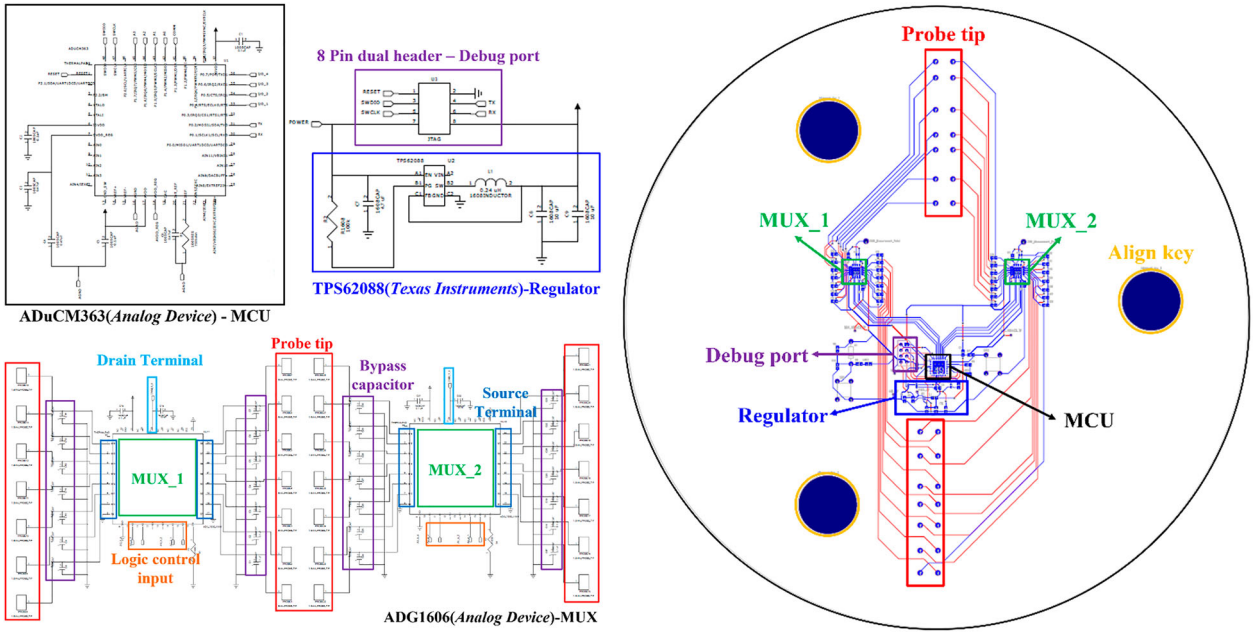

Figure 4. Measurement system logic (top) and PCB layout (bottom).

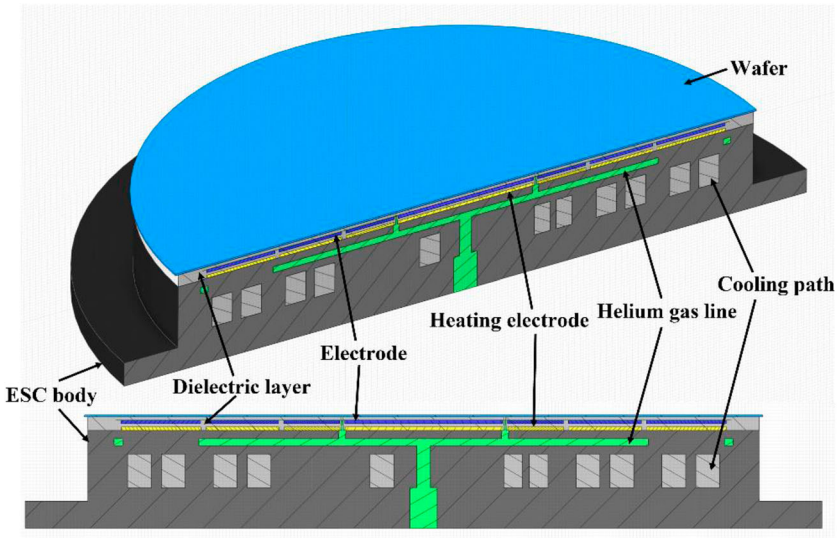

Figure 5. Structure of ESC.

power applied to the heating electrode changes with the designer. Moreover, components other than the heating electrode should be considered in the design process [19, 20]. In Figure 5, only a part of the design of the ESC heating electrode resistance measurement system is presented. The heating electrode of an ESC, which has high thermal conductivity, forms a heating electrode circuit pattern on the ceramic plate. The heating electrode circuit pattern has various forms depending on the designer, e.g. a coil pattern consisting of a twisted metal wire and a planar pattern. An ESC designer may design a heating electrode with a high heat generation rate using the resistance equation ($R = \rho L/A$) and Joule heating equation ($H = = Rt$). Furthermore, achieving high adhesion between the circuit and ceramic material, high oxidation resistance and temperature adaptability, high heating density and resistance, and low manufacturing cost must be considered in the design [21, 22].

When the resistance of the heating electrode of an ESC decreases, the current flowing into it may flow into the attached wafer, causing arcing and short circuits [23]. Moreover, metal atoms and electrons collide with each other when power is supplied to the heating electrode, and voids formed by electromigration can result in disconnection. Persistent disconnection suggests that the power supplied to the heating electrode is transmitted inappropriately, and thus effective temperature control cannot be achieved. When such problems occur, a high-accuracy DMM is required to measure the resistance of the heating electrode.

In PCS, a probe tip contacts the exposed heating electrode terminal. When power is supplied to the PCS, MCU drives, and programmes stored in the flash

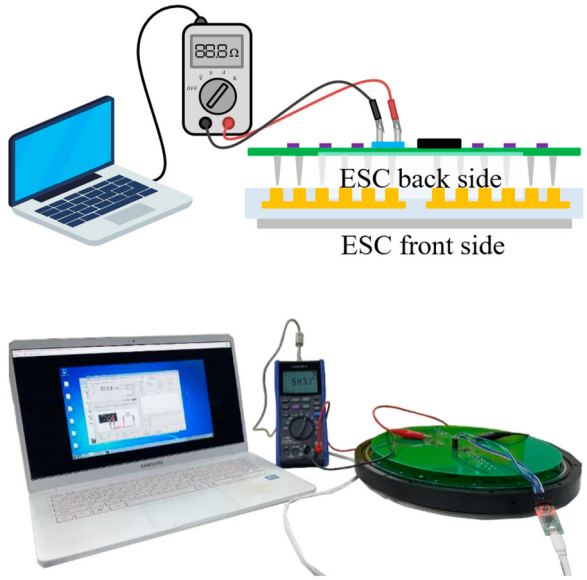

Figure 6. Schematic of ESC heating electrode resistance inspection system (top) and its connection to ESC (bottom).

memory are implemented sequentially. When receiving an input signal from a user, the MCU controls a probe tip using the MUXs and measures the resistance of the heating electrode. As the probe tip is changed, the zone of the heating electrode of the ESC to be measured changes. Because the resistance of the heating electrode is high, 15 − 20 s are required for the DMM-measured value to stabilize. Therefore, MCU controls the MUXs to change the position of the probe tip and measure the stable resistance value after 20 s. After measuring the resistance, the position of the probe tip is changed again. Figure 6 shows the experimental environment.

The software used to measure the resistance was provided by the DMM manufacturer. The resistance is measured every second, as shown in Figure 7, and saved as a comma-separated value (.csv) file after all heating zone measurements are completed. The coordinates of the heating electrode region are matched with the heating electrode recorded in the csv file. The overall resistance distribution is obtained by displaying the corresponding heating electrode resistance map. In a 144-zone ESC heating electrode region map, the heating electrode resistance value is visualized based on the minimum and maximum values. Then, the maximum, central, minimum, and average heating electrode resistance values in the heating electrode resistance map are calculated. The overall system flowchart is shown in Figure 8.

The ceramic plate of an ESC is an important part in direct contact with a wafer during the process, and there should be no particles and scratches on it. If it is damaged, wafer chucking is performed inappropriately. Therefore, it must be repaired again. Currently, as ESC parts are expensive (more than USD 20,000 per unit) [24], a method to protect the ceramic plate is required when measuring the heating electrode resistance. In this study, self-made jigs, which were used to prevent the possibility of damage to the ceramic plate of an ESC, ensured strong performance of the heating electrode. Generally, jigs are used to store wafers after the processing is complete and to minimize the effects of particles and contamination [25]. Top and bottom jigs were designed, as shown in Figure 9. The following positioning order was ensured: bottom jig, ESC, PCS, and top jig. An alignment key was used to align the heating electrode terminals of an ECS with the PCS probe tips. Once the alignment is complete, ESC and PCS are secured using the jigs with bolts (M10 × 40 mm). The top jig is fixed to the PCS board, whereas the bottom jig is fixed to the ESC ceramic plate 3.5

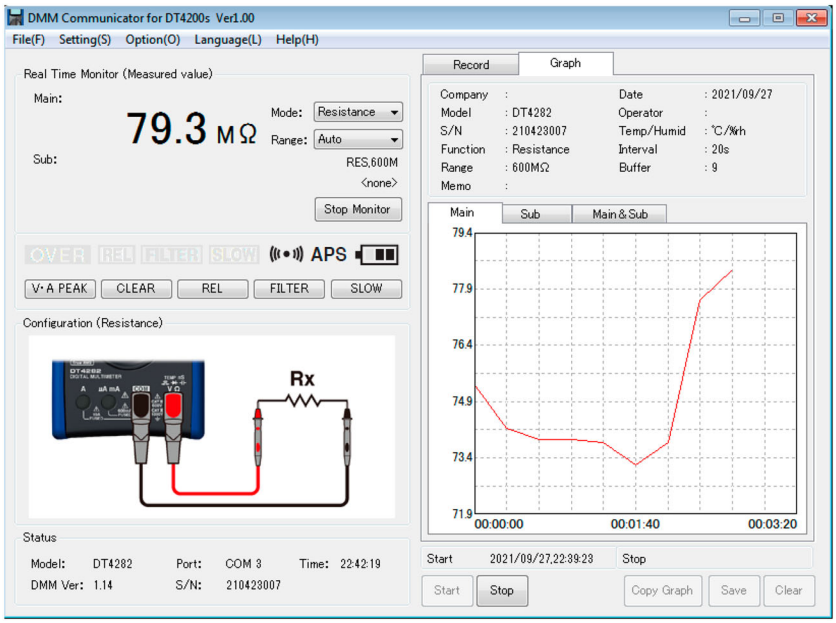

Figure 7. HIOKI's DT4282 DMM user interface software.

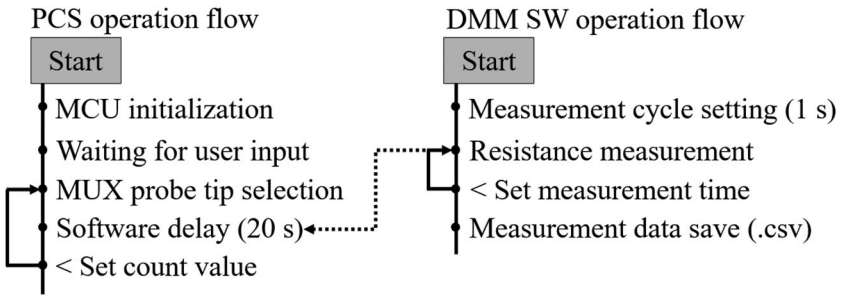

Figure 8. System operational flow.

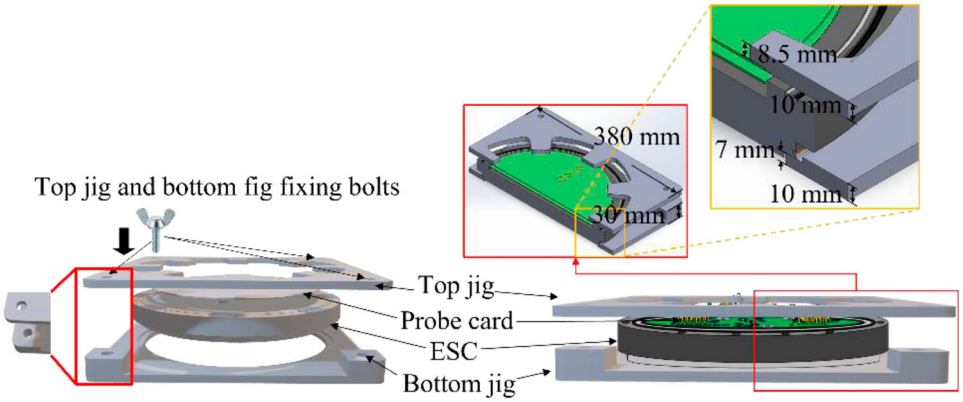

Figure 9. Jig design, 3D side view (left), and mounting schematic (right).

mm away from the bottom to protect it from particles and scratches. The manufactured jigs, as shown in Figure 10, are formed of polyether ether ketone, which has excellent insulation and chemical resistance.

Results and discussion

If a PCS measures the resistance of the heating electrode of an ESC inaccurately, it cannot diagnose the temperature control function error of the ESC. Several parasitic resistances, such as the operating resistance of the components, parasitic resistance of PCB copper wire connecting the components, and contact resistance of the probe tips, can affect the ESC heating electrode resistance measurement. Therefore, the resistance of the heating electrode of an ESC using the developed PCS was measured after experimentally verifying the PCS accuracy. Figure 11 shows the PCS accuracy verification results obtained using a standard resistor. The ESC heating electrode resistance value corresponds to high resistance. Therefore, standard resistances of 10, 40, and 100 MΩ were used. Figures 11 (a_1, b_1, and c_1) and (a_2, b_2, and c_2) show the standard resistance values measured with the PCS and using the DMM without the PCS, respectively. Figure 12 depicts the circuit for representing the component parasitic resistance, which impacts the PCS when the DMM measures the standard resistance. The on-resistance of the MUXs was 14 Ω, whereas the contact resistance of the probe tip was 20 mΩ, as per the component datasheet. The resistivity of the PCB line is given as

$$R = \frac{\rho L}{A}[1 + \{T_0 \times (T - T_{25})\}], \tag{1}$$

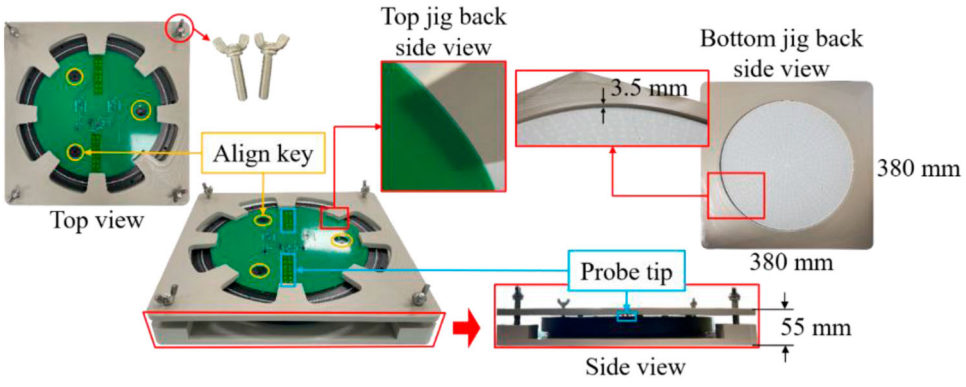

Figure 10. ESC and PCS fixed to jigs using bolts (M 10 × 40 mm).

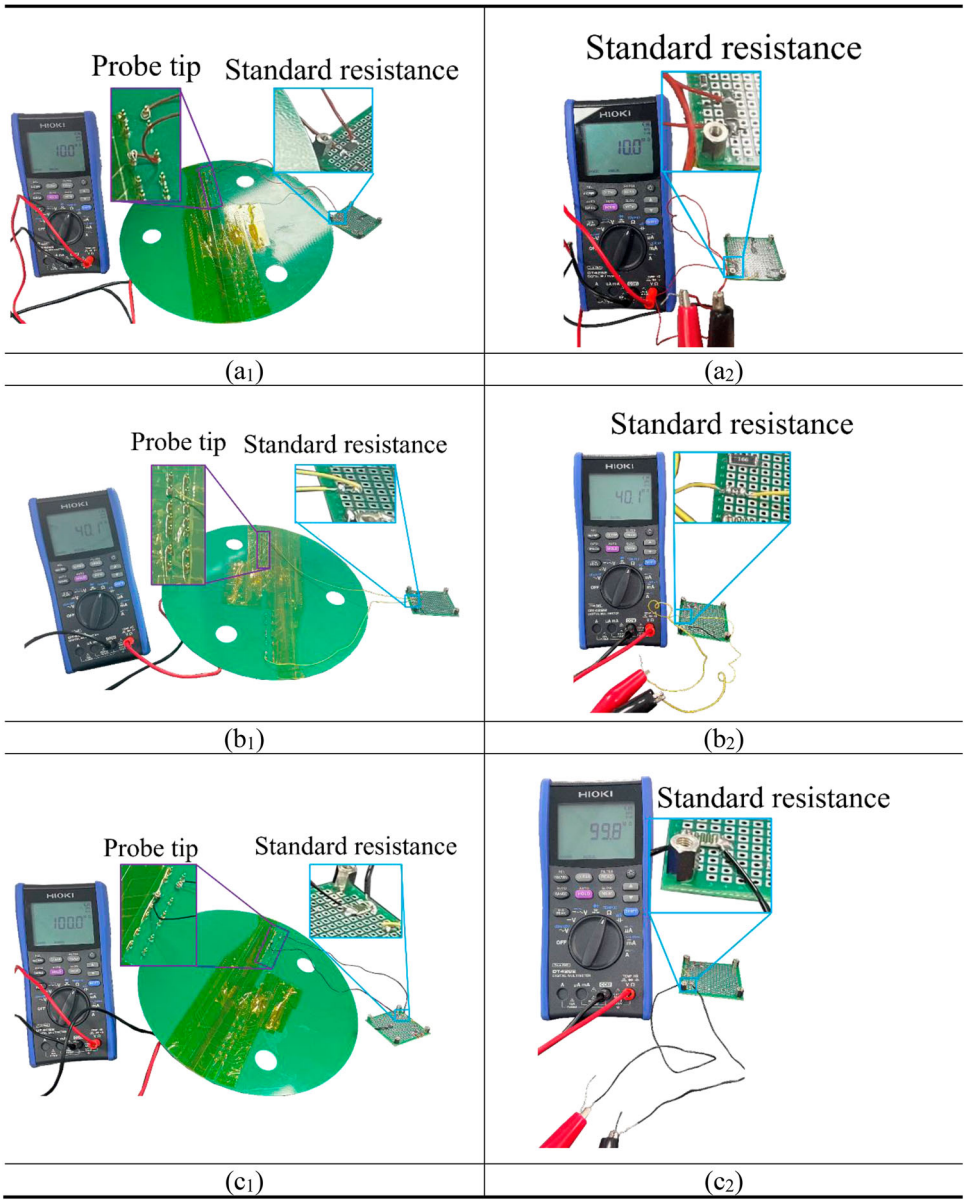

Figure 11. Standard resistance measurement results with PCS (10 MΩ (a1), 40 MΩ (b1), and 100 MΩ (c1)) and without PCS (10 MΩ (a2), 40 MΩ (b2), and 100 MΩ (c2)).

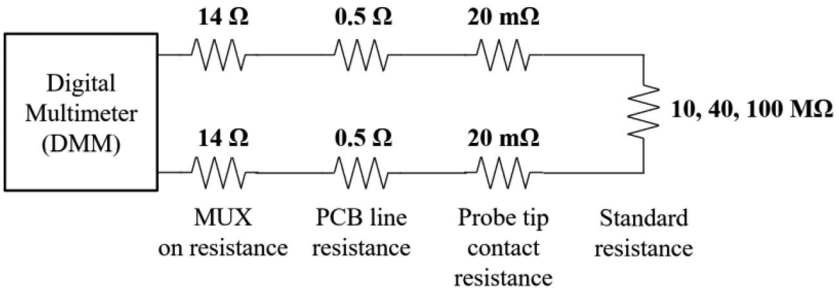

Figure 12. PCS resistive component equivalent circuit.

where ρ is the copper resistivity (1.7×10^{-6} Ωcm), L is the PCB copper line length (mm), A is the area, and T is the temperature (°C). T_0 is the copper temperature coefficient (25 °C = 3.9×10^{-3} Ω/°C), and T_{25} is 25 °C. Because the PCS is considered to be used at 25 °C and there is no temperature difference in the copper line, it is unnecessary to consider the copper temperature coefficient. A PCB line resistance of approximately 1 Ω was calculated using Eq. (1). The parasitic resistance of the components of the PCS is approximately 30 Ω, which is

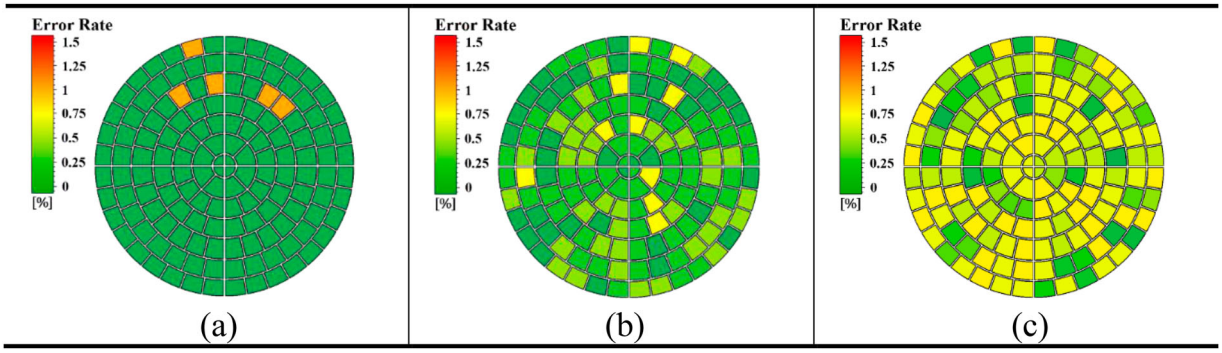

Figure 13. Standard resistance error rate distribution using PCS; (a) 10 MΩ, (b) 40 MΩ, and (c) 100 MΩ.

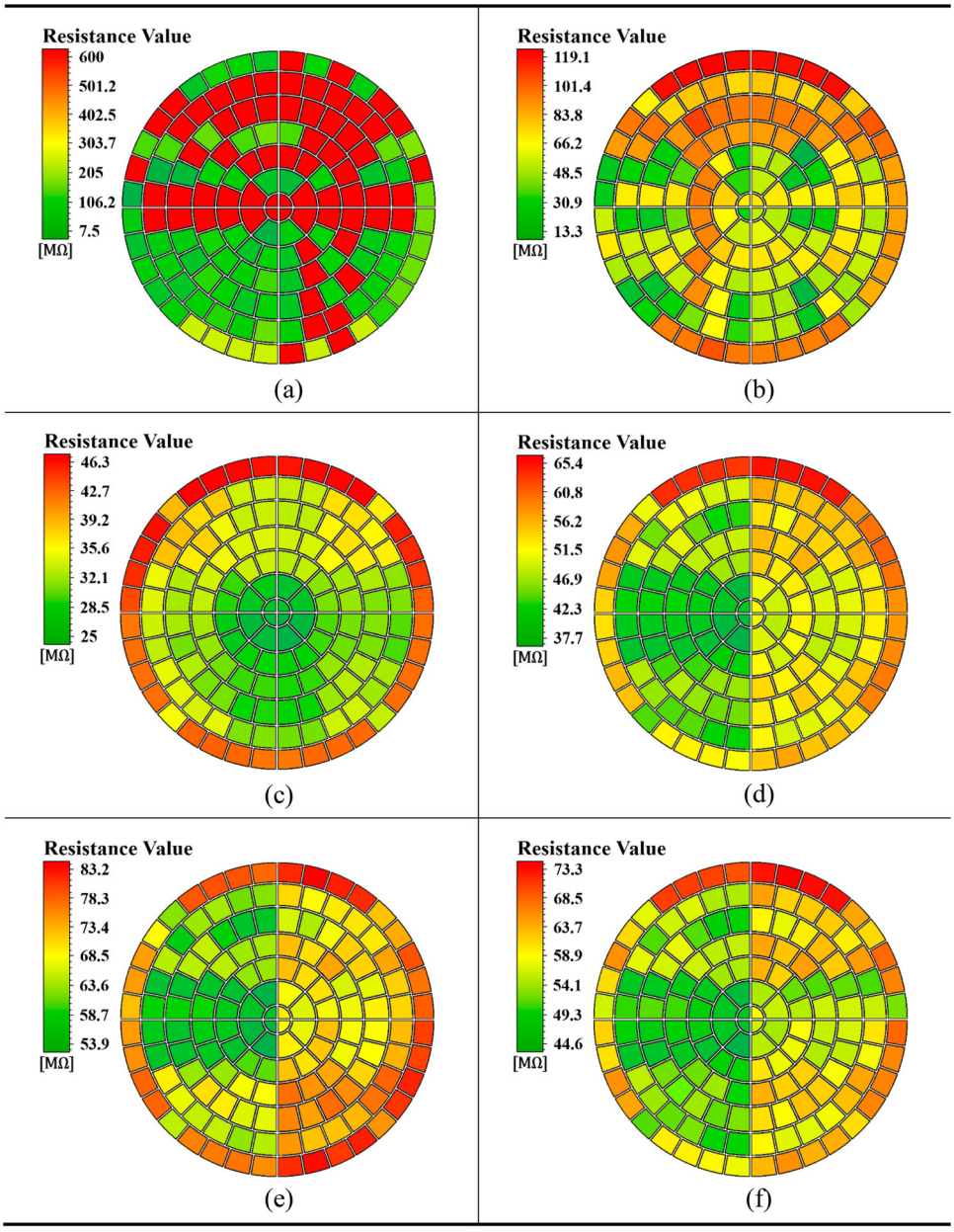

Figure 14. 144-zone ESC heating electrode resistance area maps.

smaller than the standard resistance. Therefore, it does not affect the error rate.

$$\text{Error Rate } (\%) = \frac{|\,Measured(R) - Real(R)|}{Real(R)} \times 100, \tag{2}$$

where measured (R) is the standard resistance value measured by PCS, whereas real (R) is that measured by DMM. The standard resistors shown in Figure 13(a–c) are 10, 40, and 100 MΩ (±5% tolerance), respectively. When comparing the measurement results of the PCS

Table 2. PCS error rates.

	(a)	(b)	(c)
Standard resistance value (MΩ)	10	40	100
Real resistance value (MΩ)	10	40.1	99.8
Measured resistance value (MΩ)	10.1	40.4	99
Max. error rate (%)	1	0.75	0.8

Table 3. 144-zone ESC heating electrode resistance.

	(a)	(b)	(c)	(d)	(e)	(f)
Max. (MΩ)	600	119.2	46.3	65.4	83.2	73.3
Middle. (MΩ)	303.7	66.2	35.6	51.5	68.5	58.9
Min. (MΩ)	7.5	13.2	25	37.7	53.9	44.6
Max. − Min. (MΩ)	592.4	52.9	21.2	13.8	29.3	28.7

and DMM, the maximum error rates in the 10, 40, and 100 MΩ heating electrode resistance maps were 1%, 0.75%, and 0.8%, respectively. In the test environment, errors may be due to the contact resistance when connecting the standard resistance with a probe tip, parasitic resistance of the line connecting a probe tip, and standard resistance tolerance. However, these errors were negligible compared to that of the standard resistance. Table 2 summarizes the measurement results and error rates.

In the etching process, several phenomena, such as non-uniform sheathing at the wafer edge and chemical dislocation discontinuities, cause temperature differences between the chamber and wafer [26]. Heat is transferred from high to low temperature areas owing to the radiation effect. Inside the process chamber, the centre of an ESC has a relatively higher temperature than that of the chamber wall. Therefore, heat is transferred from the former to the latter. Additionally, wafer temperature control can be improved by designing the ESC heating electrode resistance value to increase from the centre to the edge by Joule heating ($H = I^2Rt$).

The actual temperature performance evaluation requires a control unit and software of the ESC. However, these were unavailable, and the resistance was measured by separating the ESC from the equipment. Six types of 144-zone ESCs were measured, and the experiments were conducted in a clean room to prevent contamination. The standard specification for the resistance of the heating electrode of each 144-zone ESC has not been established. Figure 14(a–f) show the heating electrode resistance maps obtained after measuring the heating electrode resistance of each 144-zone ESC model using PCS. As shown in Figure 14 (a), the heating electrode resistance exceeded 600 MΩ, which is the DMM measurement limit. Consequently, the heating electrode was disconnected. If a heating electrode is disconnected, no power is supplied. Thus, the temperature control function cannot be performed, and the heating electrode must be repaired. Figure 14 (b)–(f) show a trend of increase in resistance from the centre to the edge. The value varies depending on the 144-zone ESC model and the period of use. Table 3 lists the heating electrode resistance for each 144-zone ESC model.

Conclusion

In this study, a PCS bonded to a 144-zone ESC heating electrode resistance measurement system was proposed. A maximum error rate of 1% was obtained through PCS accuracy verification experiments using a standard resistor. This value can be considered negligible because it falls within 5% of the allowable range error of standard resistors. Therefore, the heating electrode resistance measured using the PCS is reliable. The number of heating electrode zones of the ESC used in the experiment is 144. A 144-zone ESC heating electrode resistance map represents the ESC heating electrode resistance distribution. When the DMM measurement limit was exceeded, 68 heating electrode zones were disconnected. When a heating electrode was disconnected and power could not be supplied, the temperature control function could not be performed. By introducing PCS, the maintenance time was reduced by approximately 66% from 3 h to 1 h. Therefore, the maintenance efficiency was improved. Although the resistance of a heating electrode could not completely indicate the state of the ESC, the state in which the heating electrode was disconnected can be verified. Additionally, the temperature control function could not be performed. If this system is further developed to measure the voltage and current used for temperature control of the heating electrode and voltage used for wafer chucking, it will be a useful ESC inspection system that can comprehensively evaluate the status of an ESC.

Acknowledgments

This study was supported by the Materials, Components, and Equipment Research Program funded by the Gyeonggi Province (G14AICT06T10001). The authors are grateful to Mr. J.Y. Lee and Mr. J.W. Oh from the On-project Division at FST Technology for the technical discussion on prototyping. We would like to thank Editage (www.editage.co.kr) for English language editing.

Disclosure statement

No potential conflict of interest was reported by the author(s).

Funding

This work was supported by Korea Institute for Advancement of Technology (KIAT) grant funded by the Korea Government (MOTIE). (P0008458, The Competency Development Program for Industry Specialist.)

ORCID

Sang Jeen Hong http://orcid.org/0000-0002-6576-690X

References

[1] Pizzagalli A, Buisson T, Beica R. "3D technology applications market trends & key challenges," *25th SEMI Adv. Semi. Manufac. Conf.* (ASMC 2014), pp. 78–81, 2014. doi: 10.1109/ASMC.2014.6846981.

[2] Wu B, Kumar A, Pamarthy S. High-aspect ratio silicon etch: a review. J Appl Phys. 2010;108(5):108–127. doi: 10.1063/1.3474652.

[3] Zarowin CB, Horwath RS. Control of plasma etch profiles with plasma sheath electric field and rf power density. J Electrochem Soc. 1982;129(11):2541–2547. doi: 10.1149/1.2123602.

[4] Boulbar EDL, Lewins CJ, Allsopp DWE, et al. Fabrication of high-aspect ratio GaN nanostructures for advanced photonic devices. Microelectron Eng. 2016;153:132–136. doi: 10.1016/j.mee.2016.03.058.

[5] Nisha KV, Suryanarayana K, Rajaneesh A. "Modelling and simulation of multi coil induction heating system for semiconductor wafer processing," 2016 *IEEE Int. Conf. Recent Trend. Electron. Info. Commun. Technol. (RTEICT)*, pp. 588–592, 2016. doi: 10.1109/RTEICT.2016.7807890.

[6] Yamamura W. "Electrostatic chuck with built-in heater," *U.S. Patent 2006/0133004 A1*, Jun. 22, 2006. doi: patent/US20060133004.

[7] Sing H, Gaff K. "Heating plate with flat heater zones for semiconductor processing," *U.S. Patent 8,637,794 B2*, Jan. 28, 2014. doi: patent/US8637794B2.

[8] Parquet BD. "Sensor system for multizone electrostatic chucks," *U.S. Patent 10,440,777 B2*, Oct. 8, 2019. doi: patent/US10440777B2.

[9] Lee HC, Go KD. "Electrostatic chuck separated from heating means," *K.R. Patent 10-0759952*, Sep. 12, 2007. doi: patent/KR100759952B1.

[10] Thei KB, Chuang HM, Tsai SF, et al. Effects of electrical and temperature stress on polysilicon resistors for CMOS technology application. Superlattice Microst. 2002;31(6):289–296. doi: 10.1006/spmi.2002.1048.

[11] Takebayashi H, Hirata N, Hasegawa S. "Electrostatic chuck heater," *U.S. Patent 10,483,146 B2*, Nov. 19, 2019. doi: patent/US10483146B2.

[12] Min CH, Kim TS. Development and characterization of vertical type probe card for high density probing test. J Korean Ins Elec Electron Mat Eng. 2006;19(9):825–831. doi: 10.4313/JKEM.2006.19.9.825.

[13] Lee SH, Chu SI, Kim JH, et al. Reliable design and electrical characteristics of vertical MEMS probe Rip. J Appl Reliability. 2007;7(1):23–29. doi: article/JAKO200727640428661.

[14] Fu W, Chien CF, Tang L. Bayesian network for integrated circuit testing probe card fault diagnosis and troubleshooting to empower industry 3.5 smart production and an empirical study. J Intel Manufac. 2020: 1–14. doi: 10.1007/s10845-020-01680-0.

[15] Go KN, Sung JG. "Electrostatic chuck repair method," *K.R. Patent 10-2184705*, Nov. 24, 2020. doi: patent/KR102184705B1.

[16] Lubomirsky D, Sun JY, Markovsky M, et al. "Electrostatic chuck with advanced RF and temperature uniformity," *U.S. Patent 8,937,800 B2*, Jan. 20, 2015. doi: patent/US8937800B2.

[17] Blackburn DL. "Temperature measurements of semiconductor devices-a review," *20th IEEE Semi. Therm. Meas. Manage. Symp.*, pp. 70–80, 2004. doi: 10.1109/STHERM.2004.1291304.

[18] Shih H, Ullal S, Huang T, et al. "System and method for testing an electrostatic chuck," *U.S. Patent 8,143,904 B2*, 27 Mar., 2012. doi: patent/US8143904B2.

[19] Sun Y, Cheng J, Lu Y, et al. Design space of electrostatic chuck in etching chamber. J Semi. 2015;36(8):1–7. doi: 10.1088/1674-4926.

[20] Lee KS. Effect of the si-adhesive layer defects on the temperature distribution of electrostatic chuck. J Semi Disp Technol. 2012;11(2):71–74. doi: article/JAKO201207064159005.

[21] Miyata S. "Method of manufacturing an electric heating element," *U.S. Patent 6,486,447 B2*, Nov. 26, 2002. doi: patent/US6486447B2.

[22] Nasman R, Robison RL, Fujisato T. "High-temperature electrostatic chuck and method of using," *U.S. Patent 8,194,384 B2*, Jun. 5, 2012. doi: patent/US8194384B2.

[23] Morioka I, Nobori K, Kawajiri T, et al. "Electrostatic chuck with heater and manufacturing method thereof," *U.S. Patent 2008/0049374 A1*, Feb. 28, 2008. doi: patent/US20080049374A1.

[24] Sana M, Saleem U, Farooq M, et al. Identification of failure modes on electrostatic chuck through reliability centered maintenance: a case study. Proc Pak Acad Sci A. 2018;55(2):21–32. doi: PPAS-A/article/view/168.

[25] Takeshi I, Atsuo K. "Jig for semiconductor wafer and method for producing the same," *U.S. Patent 6,093,644*, Jul. 25, 2000. doi: patent/US6093644A.

[26] Hwang S, Kanarik K. Evolution of across-wafer uniformity control in plasma etch. Solid State Technol. 2016;59(5):16–20. doi: 2016/08/evolution-of-across-wafer-uniformity-control-in-plasma-etch.